# HOPF BIFURCATION OF A TWO-DEGREE-OF-FREEDOM VIBRO-IMPACT SYSTEM

G.-W. Luo, J.-H. Xie

# HOPF BIFURCATION OF A TWO-DEGREE-OF-FREEDOM VIBRO-IMPACT SYSTEM

G.-W. Luo

*Department of Mechanical Engineering, Lanzhou Railway Institute, Lanzhou* 730070, *People's Republic of China*

AND

J.-H. Xie

*Department of Applied Mechanics and Engineering, Southwest Jiaotong University, Chengdu* 610031, *People's Republic of China*

The bifurcation problem of a two-degree-of-freedom system vibrating against a rigid surface is studied in this paper. It is shown that there exist Hopf bifurcations in the vibro-impact systems with two or more degrees of freedom under suitable system parameters. In the paper, a centre manifold theorem technique is applied to reduce the Poincaré map of the vibro-impact system to a two-dimensional one, and then the theory of Hopf bifurcation of maps in $R^2$ is applied to conclude the existence of Hopf bifurcation of the vibro-impact system. The theoretical solutions are verified by numerical computations. The quasi-periodic response of the system, represented by invariant circles in the projected Poincaré sections, is obtained by numerical simulations, and routes of quasi-periodic impacts to chaos are stated briefly.

## 1. INTRODUCTION

The performance of vibrating systems with clearances between the moving components is accompanied by impact action for the moving components in a large number of diverse engineering fields. This occurs when the vibration amplitudes of some components of systems exceed critical values (clearances or gaps). Examples of these types of machines and equipment include vibration hammers, impact dampers, machinery for compacting, milling and forming, gears, shakers, wheel–rail interaction of high speed railway coaches, etc. These systems with impacts are strongly non-linear due to the existence of one or more impact pairs of components. The optimization of designs for mechanical systems with impacts must be based on an overall knowledge of the performance of vibro-impacting systems. Hence phenomena of bifurcations and chaos in vibro-impacting systems have been investigated extensively by many researchers in recent years. Much new ground has been broken in analysing and understanding the performance of vibro-impact systems. A survey of publications and results of research can be found partly in several monographs [1–25]. The dynamics of one-degree-of-freedom vibro-impact systems have been studied in great detail in references [1–15], which include bifurcations, singularities in vibro-impact systems and chaos, etc. Bifurcations and chaos have also been analysed on corresponding multi-degree-of-freedom systems in references [16–25]. However, the emphasis has been on problems of period-doubling and saddle-node bifurcations. The phenomena of Hopf bifurcations have only been investigated by a few researchers. Xie [15] investigated

codimension two bifurcations and Hopf bifurcations of a single-degree-of-freedom system vibrating against an infinite large plane. Natsiavas [22] analysed a two-degree-of-freedom piecewise linear system under harmonic excitation and obtained quasi-periodic impacts and their route to chaos by the numerical method. Ivanov [24] thought it possible for Hopf bifurcation to exist in multi-degree-of-freedom vibro-impact systems for the conjugate pair of multipliers intersecting the unit circle.

In this paper, the phenomena of Hopf bifurcation of a two-degree-of-freedom system vibrating against an infinitely large plane are analyzed in great detail. First, the Poincaré map of the vibro-impacting system is established; then a centre manifold theorem technique [26–28] is applied to reduce the Poincaré map to a two-dimensional one. By virtue of the two-dimensional map and theory of Hopf bifurcation of maps in $R^2$, which is set out in references [29] and [30], we are able to discuss the existence of Hopf bifurcation of the vibro-impacting system. Finally, the quasi-periodic response of the system, presented by invariant circles in the projected Poincaré sections, is obtained by numerical simulations, and routes of quasi-periodic impacts to chaos are stated briefly.

## 2. PERIODIC IMPACTS AND THE POINCARÉ MAP

The mechanical model for a two-degree-of-freedom vibrator with masses $M_1$ and $M_2$ is shown in Figure 1. The masses are connected to linear springs with stiffness $K_1$ and $K_2$. The excitations on both masses are harmonic with amplitudes $P_1$ and $P_2$. The mass $M_1$ impacts against a rigid surface when its displacement $X_1$ equals the gap $B$. The impact is described by a coefficient of restitution $R$, and it is assumed that the duration of impact is negligible compared to the period of the force. Between impacts, for $X_1 < B$, the differential equations of motion are

$$\begin{bmatrix} M_1 & 0 \\ 0 & M_2 \end{bmatrix} \frac{\mathrm{d}^2}{\mathrm{d}T^2} \begin{Bmatrix} X_1 \\ X_2 \end{Bmatrix} + \begin{bmatrix} K_1 & -K_1 \\ -K_1 & K_1 + K_2 \end{bmatrix} \begin{Bmatrix} X_1 \\ X_2 \end{Bmatrix} = \begin{Bmatrix} P_1 \\ P_2 \end{Bmatrix} \sin(\Omega T + \tau). \tag{1}$$

The impact equation of mass $M_1$ is

$$\dot{X}_{1+} = -R\dot{X}_{1-}, \tag{2}$$

where $\dot{X}_{1+}$ and $\dot{X}_{1-}$ represent the impacting mass velocities of approach and departure respectively. For convenience, the equations of motion (1) are rewritten in non-dimensional form for $x_1 < b$ as

$$\begin{bmatrix} 1 & 0 \\ 0 & \mu_m \end{bmatrix} \begin{Bmatrix} \ddot{x}_1 \\ \ddot{x}_2 \end{Bmatrix} + \begin{bmatrix} 1 & -1 \\ -1 & 1 + \mu_k \end{bmatrix} \begin{Bmatrix} x_1 \\ x_2 \end{Bmatrix} = \begin{Bmatrix} 1 - f_2 \\ f_2 \end{Bmatrix} \sin(\omega t + \tau), \tag{3}$$

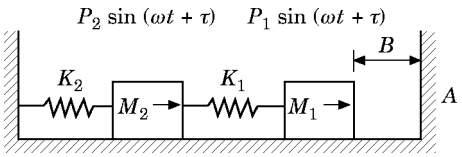


Figure 1. A schematic of the two-degree-of-freedom impact oscillator.

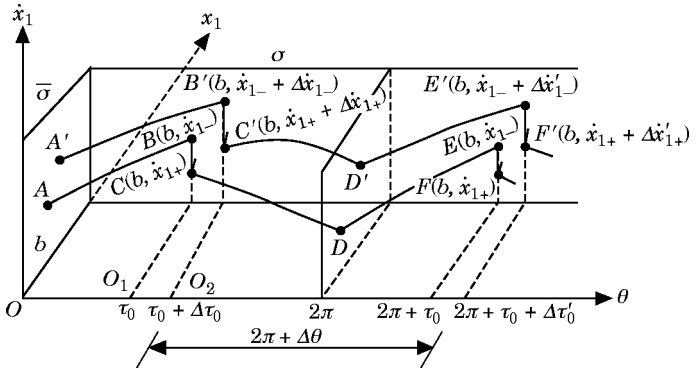


Figure 2. The stationary periodic motion ($ABCDE$) and perturbed motion ($A'B'C'D'E'$) of mass $M_1$.

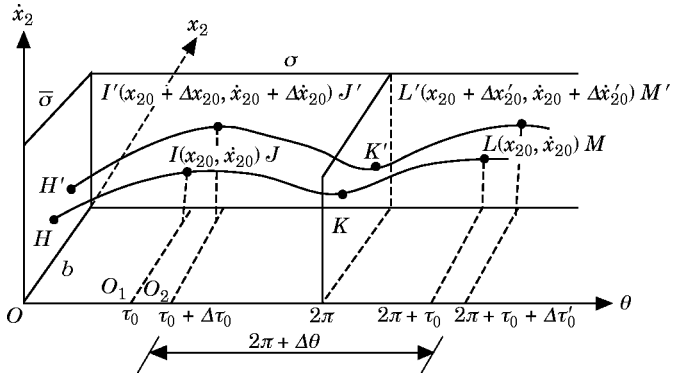


Figure 3. The stationary periodic motion ($HIJKLM$) and perturbed motion ($H'I'J'K'L'M'$) of mass $M_2$.

where the non-dimensional quantities

$$\mu_m = \frac{M_2}{M_1}, \qquad \mu_k = \frac{K_2}{K_1}, \qquad f_2 = \frac{P_2}{P_1 + P_2}, \qquad \omega = \Omega\sqrt{\frac{M_1}{K_1}}, \qquad t = T\sqrt{\frac{K_1}{M_1}},$$

$$b = \frac{BK_1}{P_1 + P_2}, \qquad x_i = \frac{X_i K_1}{P_1 + P_2} \tag{4}$$

have been introduced. In equation (3), a dot denotes differentiation with to the non-dimensional time $t$. Let $\psi$ represent the canonical model matrix of equation (3), $\omega_1$ and $\omega_2$ denote the eigenfrequencies of the system. Taking $\psi$ as a transition matrix, the equations of motion (3), under the change of variables

$$X = \psi\xi, \tag{5}$$

becomes

$$I\ddot{\xi} + \Lambda\xi = F\sin(\omega t + \tau), \tag{6}$$

where $X = (x_1, x_2)^{\mathrm{T}}$, $I$ is an unit matrix of degree $2 \times 2$, $\Lambda = \mathrm{diag}\,[\omega_1^2, \omega_2^2]$, $F = \psi^{\mathrm{T}}P$ $P = (1 - f_2, f_2)^{\mathrm{T}}$ and $\xi$ is the response of the system, in canonical co-ordinates.

The equations of motion (3) are resolved by using the formal co-ordinate and modal matrix approach. The general solution of equation (3) takes the form

$$x_i = \sum_{j=1}^{2} \psi_{ij} \, (a_j \cos \omega_j \, t + b_j \sin \omega_j \, t + A_j \sin (\omega t + \tau)), \tag{7}$$

$$\dot{x}_i = \sum_{j=1}^{2} \psi_{ij} \, (-a_j \, \omega_j \sin \omega_j \, t + b_j \, \omega_j \cos \omega_j \, t + A_j \, \omega \cos (\omega t + \tau)) \qquad (i = 1, 2), \tag{8}$$

where $\psi_{ij}$ are elements of the canonical modal matrix $\psi$, $A_j$ are the amplitude parameters and $A_j = \psi_j^{\mathrm{T}} \, P/(\omega_j^2 - \omega^2)$, $a_j$ and $b_j$ are the constants of integration, which are determined by the initial conditions and modal parameters of the system.

In the extended phase space (Figures 2 and 3), the non-smooth curves $ABCDE$ and $A'B'C'D'E'$ indicate, respectively, the periodic motion and the disturbed motion of $M_1$, and the curves $HIJKL$ and $H'I'J'K'L'$ represent, respectively, the periodic motion and the perturbed motion of mass $M_2$. The co-ordinates of the governing points on the phase orbits show the boundary and continuity conditions of the vibro-impacting system and are marked on Figures 2 and 3. We can choose a Poincaré section $\sigma \subset R^4 \times S$, where $\sigma = \{(x_1, \dot{x}_1, x_2, \dot{x}_2, \theta) \in R^4 \times S, x_1 = b\}$. By virtue of equations (2) and (3), the Poincaré map can be established as

$$\Delta X' = f(\Delta X), \tag{9}$$

where $\Delta X = (\Delta \dot{x}_1, \Delta x_2, \Delta \dot{x}_2, \Delta \tau)^{\mathrm{T}}$ and $\Delta X' = (\Delta \dot{x}_1', \Delta x_2', \Delta \dot{x}_2', \Delta \tau')^{\mathrm{T}}$ are the disturbed vectors in the hyperplane $\sigma$.

Under suitable system parameter conditions, the vibro-impact system given in Figure 1 can exhibit periodic behaviour. The periodic behavior means that if the dimensionless time $t$ is set to zero directly after an impact, it becomes $2\pi/\omega$ just before the next impact. Periodic motion corresponds to the conditions that are shown by the co-ordinate of the governing points, marked in Figures 2 and 3. After displacing the origin of the $\theta$ co-ordinate to an impact point $o_1$, we obtain

$$\begin{gathered} x_1 \, (0) = b, \qquad x_1 \, (2\pi/\omega) = b, \qquad \dot{x}_{1+} \, (0) = -R \dot{x}_{1-} \, (2\pi/\omega), \\ x_2 \, (0) = x_2 \, (2\pi/\omega), \qquad \dot{x}_2 \, (0) = \dot{x}_2 \, (2\pi/\omega), \end{gathered} \tag{10}$$

where $\dot{x}_{1-} \, (2\pi/\omega)$ is the impact velocity and $R$ is the coefficient of restitution. The first and second equations express the instantaneous nature of each impact, the third equation is the impact law, and the fourth and fifth equations express the continuity of position and velocity of mass $M_2$ at the instant of impact. Inserting the governing points into the general solution of equation (3), we can solve for the constants $a_j$ and $b_j$ of integration and the phase angle $\tau_0$ from equations (7) and (8) and express them as set out below.

If $b = 0$, then let $\tau_0 = \bar{\tau}_0$ :

$$\bar{\tau}_0 = \tan^{-1} \left( \frac{(\psi_{22} \, \psi_{11} \, s_1 \, (1 - c_2)\omega_2 - \psi_{12} \, \psi_{21} \, (1 - c_1)\omega_1) \, (1 + R)\omega}{D\omega_1 \, \omega_2 \, (1 - c_1) \, (1 - c_2) \, (1 - R)} \right); \tag{11}$$

otherwise,

$$\tau_0 = \cos^{-1} \left( \frac{\tan \bar{\tau}_0 \pm \sqrt{(\tan^2 \bar{\tau}_0 + 1)d^2 - b^2}}{(\tan^2 \bar{\tau}_0 + 1)d} \right), \tag{12}$$

$$b_1 = \frac{d\psi_{22}\,\omega(1+R)\cos\tau_0}{D\omega_1\,(1-R)}, \qquad b_2 = -\frac{\psi_{21}\,\omega_1\,b_1}{\psi_{22}\,\omega_2}, \tag{13, 14}$$

$$a_i = \frac{b_i\,s_i}{1-c_i} \qquad (i = 1, 2) \tag{15}$$

where $s_i = \sin 2\pi\omega_i/\omega$, $c_i = \cos 2\pi\omega_i/\omega$, $d = -(\psi_{11}\,A_1 + \psi_{12}\,A_2)$ and $D = |\psi|$. The $\pm$ sign means that it is possible to have two different periodic solutions under the same system parameters for the vibro-impacting system. It should be noted that the existence of periodic impacts requires equation (12) to meet the condition

$$\left|\frac{\tan\bar{\tau}_0 \pm \sqrt{(\tan^2\bar{\tau}_0 + 1)d^2 - b^2}}{(\tan^2\bar{\tau}_0 + 1)d}\right| \leqslant 1. \tag{16}$$

Otherwise, it is impossible for periodic impacts to exist. Substituting equations (11)–(15) into the general solutions of equation (3), we obtain the periodic solutions of the system shown in Figure 1, which correspond to one impact during one cycle of the forcing:

$$x_i = \sum_{j=1}^{2} \psi_{ij}\,(a_j\cos\omega_j\,t + b_j\sin\omega_j\,t + A_j\sin(\omega t + \tau_0)) \qquad (t \bmod 2\pi/\omega), \tag{17}$$

$$\dot{x}_i = \sum_{j=1}^{2} \psi_{ij}\,(-a_j\,\omega_j\sin\omega_j\,t + b_j\,\omega_j\cos\omega_j\,t + A_j\,\omega\cos(\omega t + \tau_0)) \qquad (t \bmod 2\pi/\omega). \tag{18}$$

Let us consider the perturbed motion. For simplicity of notation, we displace the origin of the $\theta$ co-ordinate to an impact point $o_2$ in Figures 2 and 3. For $\tilde{x}_1 \leqslant b$, the solutions of the perturbed motion are written in the form

$$\tilde{x}_i = \sum_{j=1}^{2} \psi_{ij}\,(\tilde{a}_j\cos\omega_j\,t + \tilde{b}_j\sin\omega_j\,t + A_j\sin(\omega t + \tau_0 + \Delta\tau)), \tag{19}$$

$$\dot{\tilde{x}}_i = \sum_{j=1}^{2} \psi_{ij}\,(-\tilde{a}_j\,\omega_j\sin\omega_j\,t + \tilde{b}_j\,\omega_j\cos\omega_j\,t + A_j\,\omega\cos(\omega t + \tau_0 + \Delta\tau)). \tag{20}$$

Inserting the coordinate of governing points $B'$ and $I'$ into equations (19) and (20), we can solve

$$\tilde{a}_1 = \frac{1}{D}\,(\psi_{22}\,b - \psi_{12}\,x_{20} - \psi_{12}\,\Delta x_{20} - DA_1\sin(\tau_0 + \Delta\tau)), \tag{21}$$

$$\tilde{a}_2 = \frac{1}{D}\,(-\psi_{21}\,b + \psi_{11}\,x_{20} + \psi_{11}\,\Delta x_{20} - DA_2\sin(\tau_0 + \Delta\tau)), \tag{22}$$

$$\tilde{b}_1 = \frac{1}{D\omega_1}\,(\psi_{22}\,\dot{x}_{1+} + \psi_{22}\,\Delta\dot{x}_{1+} - \psi_{12}\,\dot{x}_{20} - \psi_{12}\,\Delta\dot{x}_{20} - DA_1\,\omega\cos(\tau_0 + \Delta\tau)), \tag{23}$$

$$\tilde{b}_2 = \frac{1}{D\omega_2}\,(-\psi_{21}\,\dot{x}_{1+} - \psi_{21}\,\Delta\dot{x}_{1+} + \psi_{11}\,\dot{x}_{20} + \psi_{11}\,\Delta\dot{x}_{20} - DA_2\,\omega\cos(\tau_0 + \Delta\tau)). \tag{24}$$

For the disturbed motion shown in Figures 2 and 3, the dimensionless time is set to zero directly after an impact. It becomes $(2\pi + \Delta\theta)/\omega$ just before the next impact. Letting $t_e = (2\pi + \Delta\theta)/\omega$, substituting the formulas (21)–(24) and inserting the co-ordinate of governing points $E'$ and $L'$ into equations (19) and (20), we obtain

$$\sum_{i=1}^{2} \psi_{1i}\, \tilde{\xi}_i\,(t_e) = b, \tag{25}$$

$$\Delta\dot{x}'_{1+} = -R \sum_{i=1}^{2} \psi_{1i}\, \dot{\tilde{\xi}}_i\,(t_e) - \dot{x}_{1+}, \qquad \Delta x'_{20} = \sum_{i=1}^{2} \psi_{2i}\, \tilde{\xi}_i\,(t_e) - x_{20},$$

$$\Delta\dot{x}'_{20} = \sum_{i=1}^{2} \psi_{2i}\, \dot{\tilde{\xi}}_i\,(t_e) - \dot{x}_{20}, \qquad \Delta\tau' = \Delta\tau + \Delta\theta(\Delta\dot{x}_{1+}, \Delta x_{20}, \Delta\dot{x}_{20}, \Delta\tau). \tag{26}$$

Let

$$g(\Delta\dot{x}_{1+}, \Delta x_{20}, \Delta\dot{x}_{20}, \Delta\tau, \Delta\theta) = \sum_{i=1}^{2} \psi_{1i}\, \tilde{\xi}_i\,(t_e) - b, \tag{27}$$

where

$$\tilde{\xi}_i(t) = \tilde{a}_i \cos\omega_i t + \tilde{b}_i \sin\omega_i t + A_i \sin(\omega t + \tau_0 + \Delta\tau), \tag{28}$$

$$\dot{\tilde{\xi}}_i\,(t) = -\tilde{a}_i\,\omega_i \sin\omega_i t + \tilde{b}_i\,\omega_i \cos\omega_i t + A_i\,\omega \cos(\omega t + \tau_0 + \Delta\tau). \tag{29}$$

The conditions under which there exist fixed points give

$$g(\Delta\dot{x}_{1+}, \Delta x_{20}, \Delta\dot{x}_{20}, \Delta\tau, \Delta\theta)|_{(0,0,0,0,0)} = 0.$$

Suppose that $(\partial g/\partial\Delta\theta)_{(0,0,0,0)} \neq 0$. According to the implicit function theorem, the equation (27) can be solved as

$$\Delta\theta = \Delta\theta(\Delta\dot{x}_{1+}, \Delta x_{20}, \Delta\dot{x}_{20}, \Delta\tau), \qquad \Delta\theta(0, 0, 0, 0) = 0 \tag{30}$$

Inserting (30) into (26), we finally obtain the Poincaré map

$$\begin{aligned}
\Delta\dot{x}'_{1+} &= \tilde{f}_1(\Delta\dot{x}_{1+}, \Delta x_{20}, \Delta\dot{x}_{20}, \Delta\tau, \Delta\theta) \overset{Def}{=} f_1(\Delta\dot{x}_{1+}, \Delta x_{20}, \Delta\dot{x}_{20}, \Delta\tau),\\
\Delta x'_{20} &= \tilde{f}_2(\Delta\dot{x}_{1+}, \Delta x_{20}, \Delta\dot{x}_{20}, \Delta\tau, \Delta\theta) \overset{Def}{=} f_2(\Delta\dot{x}_{1+}, \Delta x_{20}, \Delta\dot{x}_{20}, \Delta\tau),\\
\Delta\dot{x}'_{20} &= \tilde{f}_3(\Delta\dot{x}_{1+}, \Delta x_{20}, \Delta\dot{x}_{20}, \Delta\tau, \Delta\theta) \overset{Def}{=} f_3(\Delta\dot{x}_{1+}, \Delta x_{20}, \Delta\dot{x}_{20}, \Delta\tau),\\
\Delta\tau' &= \Delta\tau + \Delta\theta(\Delta\dot{x}_{1+}, \Delta x_{20}, \Delta\dot{x}_{20}, \Delta\tau) \overset{Def}{=} f_4(\Delta\dot{x}_{1+}, \Delta x_{20}, \Delta\dot{x}_{20}, \Delta\tau).
\end{aligned} \tag{31}$$

Let $v = \omega$, the Poincaré map (31) can be expressed as

$$\Delta X' = f(v, \Delta X), \tag{32}$$

in which

$$\Delta X = (\Delta \dot{x}_{1+}, \Delta x_{20}, \Delta \dot{x}_{20}, \Delta\tau)^{\mathrm{T}}, \qquad \Delta X' = (\Delta \dot{x}'_{1+}, \Delta x'_{20}, \Delta \dot{x}'_{20}, \Delta\tau')^{\mathrm{T}},$$
$$f(v, \Delta X) = (f_1, f_2, f_3, f_4)^{\mathrm{T}}.$$

We expand the function $f(v, \Delta X)$ as a Taylor series in the variables $\Delta X$ and $v$:

$$f(v, \Delta X) = \sum_{p+q \geqslant 1} F_{pq}\, v^p \Delta X^q, \tag{33}$$

$$F_{pq} = \frac{1}{p!q!} \frac{\partial^{p+q} f(v, \Delta X)}{\partial v^p\, \partial \Delta X^q}\bigg|_{(v_c, 0)}, \qquad F_{p0} \equiv 0, \quad p \geqslant 1, \tag{34}$$

$$f(v, \Delta X) = F_{01}\, \Delta X + vF_{11}\, \Delta X + v^2 F_{21}\, \Delta X + F_{02}\, [\Delta X^2] + F_{03}\, [\Delta X^3] + , \ldots, \tag{35}$$

where $F_{02}$ and $F_{03}$ denote the terms of two and three respectively.

Linearizing the Poincaré map at the fixed point results in the matrix

$$Df(v, 0) = \begin{bmatrix} \frac{\partial f_1}{\partial \Delta \dot{x}_{1+}} & \frac{\partial f_1}{\partial \Delta x_{20}} & \frac{\partial f_1}{\partial \Delta \dot{x}_{20}} & \frac{\partial f_1}{\partial \Delta\tau} \\ \frac{\partial f_2}{\partial \Delta \dot{x}_{1+}} & \frac{\partial f_2}{\partial \Delta x_{20}} & \frac{\partial f_2}{\partial \Delta \dot{x}_{20}} & \frac{\partial f_2}{\partial \Delta\tau} \\ \frac{\partial f_3}{\partial \Delta \dot{x}_{1+}} & \frac{\partial f_3}{\partial \Delta x_{20}} & \frac{\partial f_3}{\partial \Delta \dot{x}_{20}} & \frac{\partial f_3}{\partial \Delta\tau} \\ \frac{\partial f_4}{\partial \Delta \dot{x}_{1+}} & \frac{\partial f_4}{\partial \Delta x_{20}} & \frac{\partial f_4}{\partial \Delta \dot{x}_{20}} & \frac{\partial f_4}{\partial \Delta\tau} \end{bmatrix}_{(v,0,0,0)}. \tag{36}$$

Let $\Delta X = (\Delta x_1, \Delta x_2, \Delta x_3, \Delta x_4)^{\mathrm{T}}$ denote $\Delta X = (\Delta \dot{x}_{1+}, \Delta x_{20}, \Delta \dot{x}_{20}, \Delta\tau)^{\mathrm{T}}$. It is easy to calculate the following derivatives in matrix (36):

$$\frac{\partial \Delta\theta}{\partial \Delta x_i} = -\frac{\partial g}{\partial \Delta x_i} \Big/ \left(\frac{\partial g}{\partial \Delta\theta}\right) \qquad (i = 1, 2, 3, 4), \tag{37}$$

$$\frac{\partial f_j}{\partial \Delta x_i} = \frac{\partial \tilde{f}_j}{\partial \Delta x_i} + \frac{\partial \tilde{f}_j}{\partial \Delta\theta} \cdot \frac{\partial \Delta\theta}{\partial \Delta x_i} \qquad (i, j = 1, 2, 3, 4). \tag{38}$$

The stability of periodic impacts can be determined by the eigenvalues of $Df(v, 0)$. If all eigenvalues of $Df(v, 0)$ are inside the unit circle, then the periodic solution is stable; otherwise, it it unstable. When the eigenvalues of $Df\,(v, 0)$ with the largest modules are on the unit circle, bifurcations occur in various ways according to their numbers and their positions on the unit circle, resulting in qualitative changes in the system dynamics. In this paper, we shall consider only the case of a single complex conjugate pair of simple non-real eigenvalues, crossing the unit circle with non-zero velocity as $v$ passes $v_c$ ; the remainder of the spectrum of $Df(v, 0)$ will be assumed to stay strictly inside the unit circle. In this case, it is possible that Hopf bifurcation may take place.

## 3. REDUCTION AND HOPF BIFURCATION OF THE POINCARÉ MAP

Let us continue to consider the Poincaré map

$$\Delta X' = f(v, \Delta X), \tag{32}$$

where $\Delta X \in R^4$, $v$ is a bifurcation parameter and $v \in R^1$. Let $\Delta X^*(v)$ be a fixed point for the system (32) for $v$ in some neighbourhood of a critical value $v = v_c$ at which $Df(v, 0)$ satisfies the following assumptions:

(H1) $Df(v, 0)$ has a pair complex conjugate eigenvalues $\lambda_1$, $\lambda_2$ on the unit circle, and the other eigenvalues $\lambda_3$, $\lambda_4$ stay inside the unit circle;

$$\text{(H2)} \quad \lambda_1^m(v_c) \neq 1, \qquad m = 1, 2, 3, 4, 5;$$

$$\text{(H3)} \quad \left.\frac{\mathrm{d}|\lambda_1(v)|}{\mathrm{d}v}\right|_{v=v_c} > 0.$$

Let $r_i$ denote the eigenvector of $Df(v, 0)$ corresponding to $\lambda_i(v)$ $(i = 1, 2, 3, 4)$. If $r_3$ and $r_4$ are a complex conjugate pair of non-real eigenvectors, then let eigenmatrix $P = (\mathrm{Re}\, r_1, -\mathrm{Im}\, r_1, \mathrm{Re}\, r_3, -\mathrm{Im}\, r_3)$; otherwise, let $P = (\mathrm{Re}\, r_1, -\mathrm{Im}\, r_1, r_3, r_4)$. For all $v$ in some neighbourhood of $v_c$, the map (32), under the change of variables

$$\Delta X = \Delta X^* + PY, \qquad v = v_c + \mu, \tag{39}$$

becomes

$$Y' = F(\mu, Y), \tag{40}$$

where $DF(\mu, 0)$ has the form

$$DF(\mu, 0) = \begin{bmatrix} \alpha & -\omega & \\ \omega & \alpha & \\ & & D \end{bmatrix}, \tag{41}$$

in which $\alpha = \mathrm{Re}\,\lambda_1(v_c + \mu)$, $\omega = \mathrm{Im}\,\lambda_1(v_c + \mu)$ and $D$ is a real matrix with eigenvalues $\lambda_3$ and $\lambda_4$.

Let $z = y_1 + \mathrm{i}y_2$, $W = (y_3, y_4)^{\mathrm{T}}$, $G = F_1 + \mathrm{i}F_2 - \lambda z$, $\lambda = \lambda(\mu) = \alpha + \mathrm{i}\omega$, $H = (F_3, F_4)^{\mathrm{T}} - DW$ and let us show that the map (40) may be written in the form

$$z' = \lambda z + G(z, \bar{z}, W; \mu), \qquad W' = DW + H(z, \bar{z}, W; \mu). \tag{42}$$

For the system (42), there exists a local centre manifold [27], given by

$$W = W(z, \bar{z}; \mu), \tag{43}$$

on which the local behaviour of the system (42) can be reduced, by substituting equation (43) to equation (42), to a two-dimensional map. In order to determine the centre manifold $W(z, \bar{z}; \mu)$, we have to expand $W(z, \bar{z}; \mu)$ in a Taylor series about $(0, 0, \mu)$ and solve the equation

$$\begin{aligned} W(\lambda z + G(z, \bar{z}, W(z, \bar{z}; \mu); \mu), \bar{\lambda}\bar{z} + \bar{G}(z, \bar{z}, W(z, \bar{z}; \mu); \mu); \mu) \\ = DW(z, \bar{z}; \mu) + H(z, \bar{z}, W(z, \bar{z}; \mu); \mu). \end{aligned} \tag{44}$$

The Taylor series expansion of $W(z, \bar{z}; \mu)$ about $(0, 0, \mu)$ is expressed as

$$W(z, \bar{z}; \mu) = \sum_{i+j=2}^{L} W_{ij}(\mu) \frac{z^i \bar{z}^j}{i!j!} + O(|z|^{L+1}). \tag{45}$$

By substituting equation (45) into equation (44) and solving equation (44) for $W_{ij}$, we can

obtain

$$W_{ij} = (\lambda^i \overline{\lambda}^j - D)^{-1} H_{ij} \qquad (i + j = 2),$$

$$W_{30} = (\lambda^3 - D)^{-1}(H_{30} + 3H_{10}^1 W_{20} - 3\lambda G_{20} W_{11} - 3\lambda G_{20} W_{20}),$$

$$W_{21} = (\lambda^2 \overline{\lambda} - D)^{-1}(H_{01}^1 W_{20} + 2H_{10}^1 W_{11} - \overline{\lambda} G_{20} W_{11} - 2\lambda G_{11} W_{20} - 2\lambda \overline{G}_{11} W_{11} - \overline{\lambda} \overline{G}_{02} W_{02} + H_{21}),$$

$$W_{12} = \overline{W}_{21}, \qquad W_{03} = \overline{W}_{30}, \tag{46}$$

where $W_{ij}$, $G_{ij}$ and $H_{ij}$ denote $W_{ij}(\mu)$,$G_{ij}(\mu)$ and $H_{ij}(\mu)$ respectively:

$$G_{ij} = \frac{\partial^2 G}{\partial z^i \, \overline{\partial} z^j}\bigg|_{(0,0,0;\mu)}, \qquad H_{ij} = \frac{\partial^2 H}{\partial z^i \, \overline{\partial} z^j}\bigg|_{(0,\,0,\,0,\,\mu)}. \tag{47, 48}$$

$$H_{10}^1 = \frac{\partial}{\partial z}\left(\frac{\partial H}{\partial w_1}, \quad \frac{\partial H}{\partial w_2}\right)\bigg|_{(0,0,0;\mu)}, \qquad H_{01}^1 = \frac{\partial}{\partial z}\left(\frac{\partial H}{\partial w_1}, \quad \frac{\partial H}{\partial w_2}\right)\bigg|_{(0,0,0;\mu)}. \tag{49}$$

Inserting equation (45) into equation (44), we have

$$W(z, \bar{z}; \mu) = \sum_{i+j=2}^{3} W_{ij}(\mu) \frac{z^i \bar{z}^j}{i!j!} + O(|z|^4). \tag{50}$$

Let

$$z' = \lambda z + g(z, \bar{z}; \mu), \tag{51}$$

where

$$g(z, \bar{z}; \mu) = G(z, \bar{z}, W(z, \bar{z}; \mu); \mu). \tag{52}$$

The expanded form of $g(z, \bar{z}; \mu)$ is given by

$$g(z, \bar{z}; \mu) = \sum_{i+j=2}^{L} g_{ij}(\mu) \frac{z^i \bar{z}^j}{i!j!} + O(|z|^{L+1}). \tag{53}$$

Introducing equation (53) into equation (51), we obtain

$$g_{ij} = G_{ij}, \quad (i + j = 2), \quad g_{30} = G_{30} + 3G_{10}^1 W_{20}, \quad g_{21} = G_{21} + 2G_{10}^1 W_{11} + G_{01}^1 W_{20} \tag{54}$$

in which

$$G_{10}^1 = \frac{\partial}{\partial z}\left(\frac{\partial G}{\partial w_1}, \quad \frac{\partial G}{\partial w_2}\right)\bigg|_{(0,0,0;\mu)}, \qquad G_{01}^1 = \frac{\partial}{\partial \bar{z}}\left(\frac{\partial G}{\partial w_1}, \quad \frac{\partial G}{\partial w_2}\right)\bigg|_{(0,0,0,\mu)}. \tag{55}$$

The map (32) has been reduced to a two-dimensional one by using a centre manifold theorem technique [26, 27]. The two-dimensional map is expressed as

$$z' = \lambda z + \sum_{i+j=2}^{3} g_{ij}(\mu) \frac{z^i \bar{z}^j}{i!j!} + O(|z|^4). \tag{56}$$

Using the map (56) and applying the following lemma, we can discuss the existence of Hopf bifurcation for the map (32) as $v$ passes through $v_c$.

*Lemma* [29, 30]. Let $\Phi_\mu$ be a one-parameter family of diffeomorphisms on $R^2$, satisfying the following conditions:

$$\text{(C1)}\ \ \Phi_\mu(0,0) = (0,0) \qquad \text{for all } \mu;$$

$$\text{(C2)}\ \ D\Phi_\mu(0,0) \text{ has two conjugated eigenvalues } \lambda_0, \overline{\lambda}_0 \qquad \text{with } |\lambda_0| = |\overline{\lambda}_0| = 1;$$

$$\text{(C3)}\ \ d|\lambda(\mu)|/d\mu|_{\mu=0} > 0;$$

$$\text{(C4)}\ \ \lambda^m(0) \neq 1, \qquad m = 1, 2, 3, 4, 5.$$

Subject to assumptions (C1)–(C4). We can make a smooth $\mu$-dependent change of co-ordinate bring $\Phi_\mu$ into the form

$$\Phi_\mu(y_1, y_2) = N\Phi_\mu(y_1, y_2) + O(|Y|)^5. \tag{57}$$

In polar co-ordinates,

$$N\Phi_\mu = (|\lambda(\mu)|r - f_1(\mu)r^3,\ \varphi + \theta(\mu) + f_3(\mu)r^3). \tag{58}$$

If $f_1(0) > 0 (f_1(0) < 0)$, $\Phi_\mu$ has an attracting (repelling) invariant circle for $\mu > 0$ ($\mu < 0$). Suppose that the complex form of $\Phi_0$ is

$$\Phi_0(z) = \lambda_0 z + \sum_{i+j=2}^{3} g_{ij}(0)\frac{z^i\bar{z}^j}{i!j!} + O(|z|^4); \tag{59}$$

then

$$f_1(0) = \mathrm{Re}\left[\frac{(1-2\lambda_0)\overline{\lambda}_0}{2(1-\lambda_0)} g_{20} g_{11}\right] + \tfrac{1}{2}|g_{11}|^2 + \tfrac{1}{4}|g_{02}|^2 - \mathrm{Re}\left(\frac{\overline{\lambda}_0 g_{21}}{2}\right). \tag{60}$$

where $\lambda_0 = \lambda(0)$.

If the assumptions (H1)–(H3) hold for the Poincaré map, it is easy to show that the map (56) satisfies these conditions (C1)–(C4). It is not difficult to choose a set of system parameters for the vibro-impacting model shown in Figure 1 under which the Poincaré map (32) satisfies the assumptions (H1)–(H3). By computing $f_1(0)$, we can conclude the existence of an invariant circle for the map (56) and its stability in terms of the sign of $f_1(0)$. Because on the centre manifold (43) the local behaviour of the Poincaré map can be reduced to the two-dimensional one (56), it is certain that if the map (56) has an attracting (repelling) invariant circle for $\mu > 0$ ($\mu < 0$), a supercritical (subcritical) Hopf bifurcation will take place for the vibro-impacting system (32) at $v = v_c$.

## 4. EXAMPLES AND NUMERICAL SIMULATIONS

In this section the analysis developed in the former section is verified by the presentation of results for the vibro-impacting system given in Figure 1. A system with $\mu_m = 2$, $\mu_k = 5$, $f_2 = 0$, $b = 1{\cdot}5$ and $R = 0{\cdot}8$ has been chosen for analysis. $v$ is taken as a bifurcation parameter and the eigenvalues of $Df(v, 0)$ corresponding to $v$ on the interval [0·7219, 0·7396] are computed. The variation of the eigenvalues of $Df(v, 0)$ as $v$ varies on the interval, are shown in Figure 4. When $v$ increases on the interval [0·7219, 0·7368), all eigenvalues stay strictly inside the unit circle. With $|\lambda_{1,2}(v)|$ increasing and $|\lambda_{3,4}(v)|$ decreasing, $Df(v, 0)$ has a complex conjugate pair of eigenvalues $\lambda_1$, $\lambda_2$ on the unit circle

for $v = v_c = 0{\cdot}7368$; the remainder of the eigenvalues are still inside the unit circle. A pair of eigenvalues $\lambda_1$, $\lambda_2$ will cross the unit circle, and the other eigenvalues will still stay inside the unit circle, as $v$ passes through $v_c$. $v_c$ is a Hopf bifurcation value at which the map (56) satisfies the conditions (C1)–(C4). By virtue of formulae (A3) and (60), we obtain

$$\left.\frac{\mathrm{d}|\lambda_1(v)|}{\mathrm{d}v}\right|_{v=v_c} = \left.\frac{\mathrm{d}|\lambda_1(\mu)|}{\mathrm{d}\mu}\right|_{\mu=\mu_c} = 3{\cdot}0701, \qquad f_1(0) = 1{\cdot}361.$$

For the results mentioned above, we can conclude that under the chosen system parameters the map (56) has an attracting invariant circle for $\mu > 0$. This means that a supercritical Hopf bifurcation occurs for the vibro-impacting system (31), with the same system parameters. This conclusion conforms with the digital simulation results below.

The projected Poincaré sections for the vibro-impacting system are shown in Figures 5 and 6. The Poincaré section is taken in the form $\{(x_1, \dot{x}_1, x_2, \dot{x}_2, \theta) \in R^4 \times S, x_1 = b\}$. As expected, a quasi-periodic response, represented by the attracting invariant circles of Figures 5 and 6, appears at $v = 0{\cdot}7369$, just after the Hopf bifurcation value of $v = 0{\cdot}7368$. Taking a theoretical fixed point of the system corresponding to $v = 0{\cdot}7369$ as an initial map point, we obtain the attracting invariant circles shown in Figure 5 by analysing the vibro-impacting system shown in Figure 1 for 5000 impacts. The invariant circles shown in Figure 6 are obtained by taking a point outside the circles shown in Figure 5 as an initial map point and analysing the system for 4000 impacts. As the value of $v$ moves further away from the Hopf bifurcation value, the circles expand. A single torus doubling begins to occur as the value of $v$ passes through $v = 0{\cdot}7438$. Any further observable torus doubling is not founded in digital simulations. The torus doubling at $v = 0{\cdot}744$ is plotted in Figure 7. Following some single torus doubling, the system settles into chaotic motion (Figures 8 and 9).

There exists another route by which Hopf bifurcation leads to chaos in the vibro-impacting system shown in Figure 1. This route is characterized by a phenomenon in which the system settles into chaotic motion without a single torus doubling but with a quasi-attracting circle (attracting inside the circle and repelling outside it). In order to study such a case, we analyze the vibro-impacting system with a set of system parameters $\mu_m = 4$, $\mu_k = 2$, $f_2 = 0$, $b = 1{\cdot}8$ and $R = 0{\cdot}8$. The conjugate pair of eigenvalues intersecting the unit circle are shown in Figure 10. The intersecting velocity of the eigenvalues passing through the unit circle and $f_1(0)$ are

$$\left.\frac{\mathrm{d}|\lambda_1(v)|}{\mathrm{d}v}\right|_{v=v_c} = \left.\frac{\mathrm{d}|\lambda_1(\mu)|}{\mathrm{d}\mu}\right|_{\mu=\mu_c} = 0{\cdot}641, \qquad f_1(0) = 1{\cdot}096.$$

It is concluded by the same method that a supercritical Hopf bifurcation takes place for the system under the second set of chosen system parameters at $v = v_c = 0{\cdot}4906$. A single torus doubling is not observed in the numerical analysis. There are single attracting invariant circles in all projected Poincaré sections up to $v = 0{\cdot}4943$. In Figure 11 is plotted an attracting invariant circle at $v = 0{\cdot}4917$. When $v = 0{\cdot}4944$, the invariant circle becomes attracting inside the circle and repelling outside it. We take a theoretical fixed point corresponding to $v = 0{\cdot}4944$ as the initial condition and analyse the system for 4000 impacts. When the system is analysed for 1112 impacts, a large transition of phase angle occurs and the vibro-impacting system settles into chaotic motion (Figure 12).

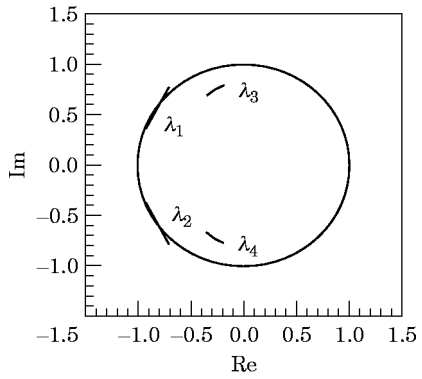


Figure 4. The conjugate pair of eigenvalues intersecting the unit circle; $v$ varies on the interval [0·7219, 0·7396].

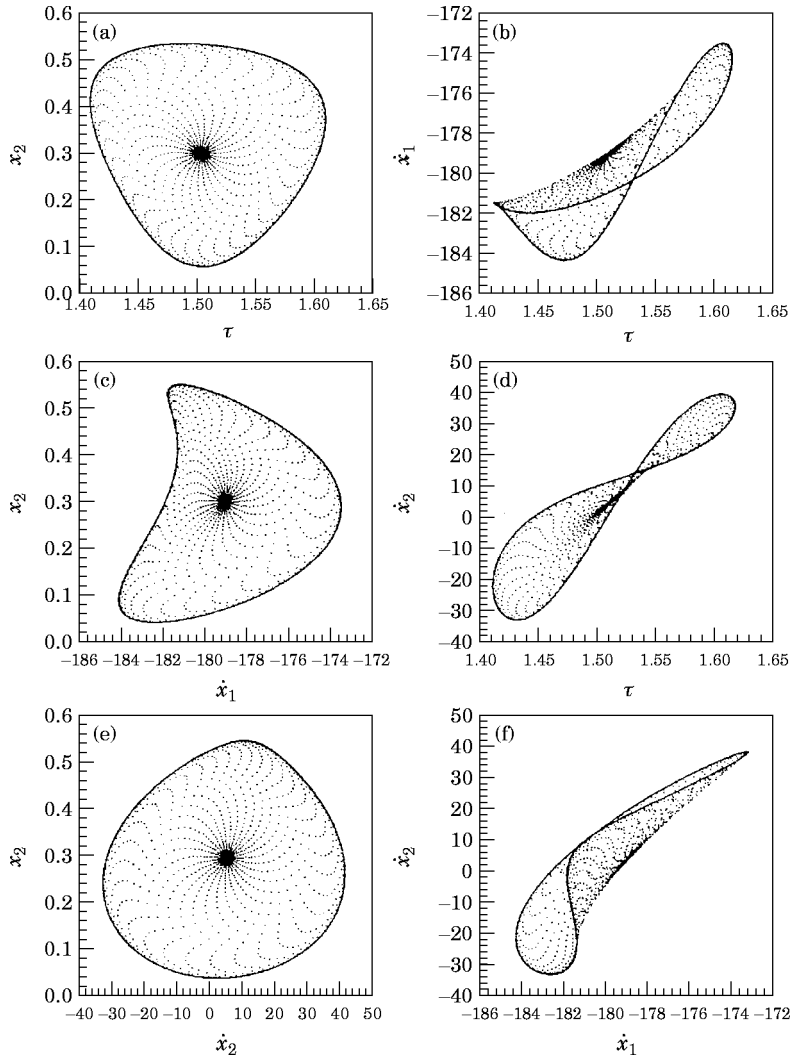


Figure 5. The quasi-periodic response of the vibro-impact system shown in projected Poincaré sections: $\mu_m = 2$, $\mu_k = 5$, $f_2 = 0$, $b = 1{\cdot}5$, $R = 0{\cdot}8$, $v = 0{\cdot}7369$.

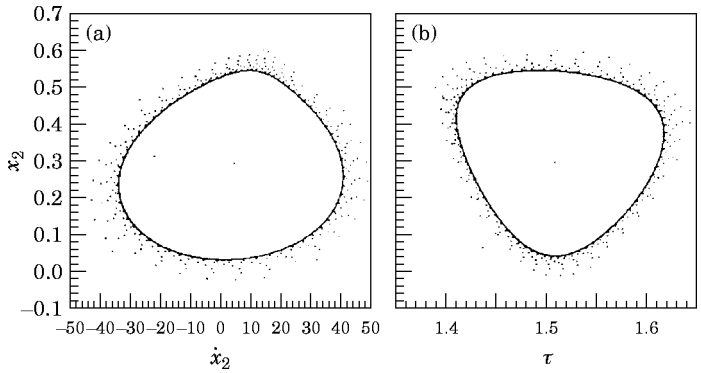


Figure 6. The quasi-periodic response of the vibro-impact shown in projected Poincaré sections: $\mu_m = 2$, $\mu_k = 5$, $f_2 = 0$, $b = 1{\cdot}5$, $R = 0{\cdot}8$, $v = 0{\cdot}7369$.

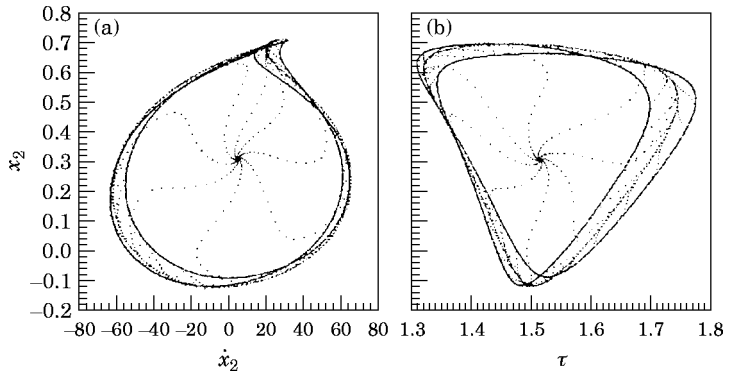


Figure 7. The torus doubling of the vibro-impact system shown in projected Poincaré sections: $\mu_m = 2$, $\mu_k = 5$, $f_2 = 0$, $b = 1{\cdot}5$, $R = 0{\cdot}8$, $v = 0{\cdot}744$.

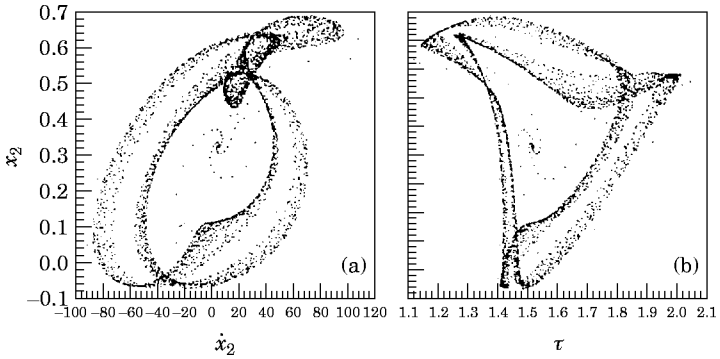


Figure 8. The chaotic motion of the vibro-impact system shown in projected Poincaré sections: $\mu_m = 2$, $\mu_k = 5$, $f_2 = 0$, $b = 1{\cdot}5$, $R = 0{\cdot}8$, $v = 0{\cdot}7519$.

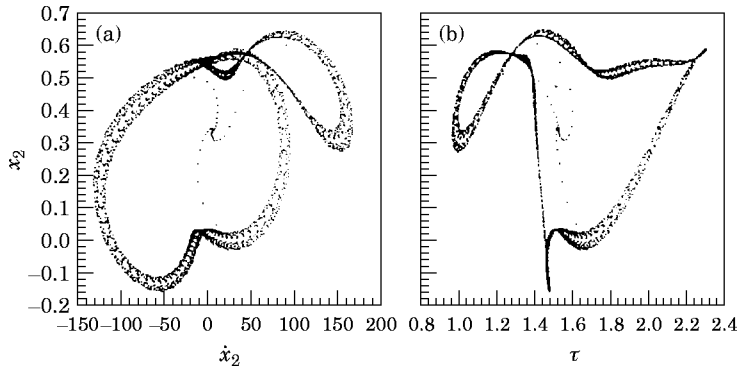


Figure 9. The chaotic motion of the vibro-impact system shown in projected Poincaré sections: $\mu_m = 2$, $\mu_k = 5$, $f_2 = 0$, $b = 1{\cdot}5$, $R = 0{\cdot}8$, $v = 0{\cdot}7555$.

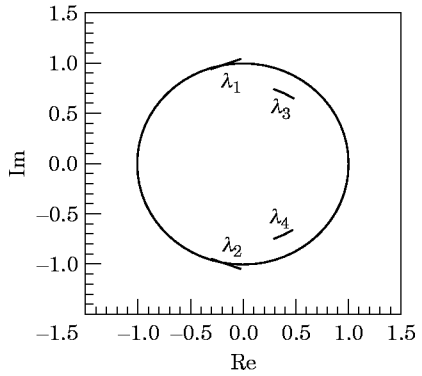


Figure 10. The conjugate pair of eigenvalues intersecting the unit circle; $v$ varies on the interval [0·458, 0·492].

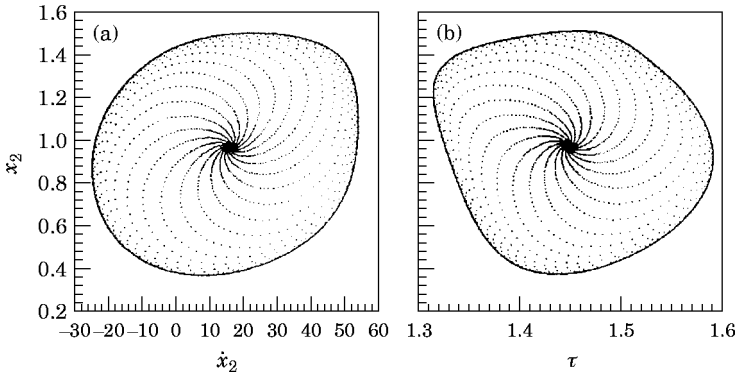


Figure 11. The quasi-periodic response of the vibro-impact system shown in projected Poincaré sections: $\mu_m = 4$, $\mu_k = 2$, $f_2 = 0$, $b = 1{\cdot}8$, $R = 0{\cdot}8$, $v = 0{\cdot}4917$.

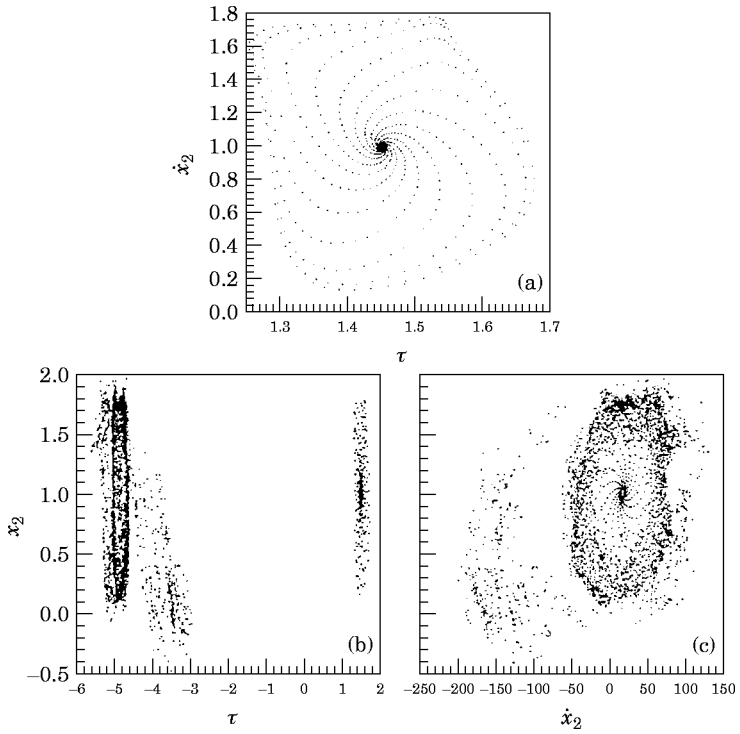


Figure 12. The chaotic motion of the vibro-impact system shown in projected Poincaré sections: $\mu_m = 4$, $\mu_k = 2$, $f_2 = 0$, $b = 1{\cdot}8$, $R = 0{\cdot}8$, $v = 0{\cdot}4944$. (a) The system is analysed for 1112 impacts from theoretical fixed point; (b, c) the system is analysed for 4000 impacts from a theoretical fixed point.

## 5. DISCUSSION

It is certain that Hopf bifurcations exist in a vibro-impacting system with two or more degrees of freedom under suitable system parameters. We have observed quasi-periodic impacts of the system shown in Figure 1 by theoretical analysis and numerical simulations. The method stated in the paper can be applied to other vibro-impacting models with two degrees of freedom, to confirm the existence of Hopf bifurcations (quasi-periodic impacts) in them. The method is effective for vibro-impact systems with two degrees of freedom. Because of the rapid increase in the number of equations, it becomes complicated to expand the Poincaré map as a Taylor series in the variables $\Delta X$ and $v$, and so the method also becomes difficult to apply. Since the degenerated case of Hopf bifurcation does not easily appear in engineering and practical applications, in general we may still analyse quasi-periodic impacts of vibro-impacting systems with more than two degrees of freedom by virtue of the satisfaction of the three assumptions (H1)–(H3) and numerical simulations. We have stated briefly the routes of quasi-periodic impacts to chaos in the former section. Two routes of quasi-periodic impacts to chaos are often observed in our numerical analyses, the former of which is analogous to the explanation in references [31] and [32]. It is necessary to make a further theoretical study of routes of quasi-periodic impacts to chaos.

## ACKNOWLEDGMENT

This work was supported by the National Science Foundation of the People's Republic of China (19672052) and the Provincial Science Foundation of Gansu, China (ZR-97-039).

## REFERENCES


1. E. H. Dowell 1982 *Journal of Sound and Vibration* **85**, 333–344. Flutter of a buckled plate as an example of chaotic motion of a deterministic autonomous system.
2. S. W. Shaw and P. J. Holmes 1983 *Journal of Sound and Vibration* **90**, 129–155. A periodically forced piecewise linear oscilinear.
3. J. M. T. Thompson 1883 *Proceedings of the Royal Society of London* **A387**, 407–427. Complex dynamics of compliant offshore structures.
4. S. W. Shaw and P. J. Holmes 1983 *Journal of Applied Mechanics* **50**, 894–857. A periodically forced impact oscillator with large dissipation.
5. S. W. Shaw 1985 *Journal of Applied Mechanics* **52**, 453–646. The dynamics of a harmonically excited system having rigid amplitude constraints.
6. G. S. Whiston 1987 *Journal of Sound and Vibration* **115**, 303–319. The vibro-impact response of a harmonically excited and preloaded one-dimensional linear oscillator.
7. G. S. Whiston 1987 *Journal of Sound and Vibration* **118**, 395–429. Global dynamics of a vibro-impact oscillator.
8. A. B. Nordmark 1991 *Journal of Sound and Vibration* **145**, 279–297. Non-periodic motion caused by grazing incidence in an impact oscillator.
9. G. S. Whiston 1992 *Journal of Sound and Vibration* **152**, 427–460. Singularities in vibro-impact dynamics.
10. S. Nsatsiava and H. Gonzalez 1992 *Journal of Applied Mechanics* 59, 284–290. Vibration of harmonically excited oscillators with asymmetric constraints.
11. F. Peterka and J. Vcacik 1992 *Journal of Sound and Vibration* **154**, 95–115. Transition to chaotic motion in mechanically stems with impacts.
12. L. Zuo and A. Curnier 1994 *Journal of Sound and Vibration* **174**, 289–313. Non-linear real and complex modes of conewise linear systems.
13. S. Narayanan and P. Sekar 1995 *Journal of Sound and Vibration* **184**, 281–298. Periodic and chaotic responses of sdf system with piecewise linear stiffness subjected to combined harmonic and flow induced excitations.
14. C. Budd and F. Dux 1995 *Journal of Sound and Vibration* **184**, 475–502. The effect of frequency and clearance variations on single-degree-of-freedom impact oscillators.
15. J.-H. Xie 1996 *Applied Mathematics and Mechanics* **17**, 65–75. Codimension two bifurcations and hopf bifurcations of an impacting vibrating system.
16. C. N. Bapat and C. Bapat 1988 *Journal of Sound and Vibration* **120**, 53–61. Impact-pair under periodic excitation.
17. M. S. Heiman, A. K. Bajaj and P. J. Sherman 1988 *Journal of Sound and Vibration* **124**, 55–78. Periodic motions and bifurcations in dynamics of an inclined impact pair.
18. J. E. Kozol and R. M. Brach 1991 *Journal of Sound and Vibration* **148**, 319–327. Two-dimensional vibratory impact and chaos.
19. Z.-Z. Shu 1991 *Acta Mechanica Sinica* **7**(4), 369–375. Motion types and chaos of multi-body systems vibrating with impacts.
20. C. K. Sung and W. S. Yu 1992 *Journal of Sound and Vibration* **158**, 317–329. Dynamics of harmonically excited impact damper: bifurcations and chaotic motion.
21. J. O. Aidanpaa and R. B. Gupta 1993 *Journal of Sound and Vibration* **165**, 305–327. Periodic and chaotic behaviour of a threshold-limited two-degree-of-freedom system.
22. S. Natsiavas 1993 *Journal of Sound and Vibration* **165**, 439–453. Dynamics of multiple-degree-of-freedom oscillators with colliding components.
23. A. P. Ivanon 1993 *Journal of Sound and Vibration* **178**, 361–378. Impact oscillations: linear theory of stability and bifurcations.
24. R. P. S. Han and A. C. J. Luo 1995 *Journal of Sound and Vibration* **181**, 231–250. Chaotic motion of a horizontal impact pair.
25. C. N. Bapat 1995 *Journal of Sound and Vibration* **184**, 417–427. The general motion of an inclined impact damper with friction.
26. B. D. Hassard, N. D. Kazarinoff and Y.-H. Wan *Theory and Applications of Hopf Bifurcation*. Cambridge: Cambridge University Press.
27. J. Car *Applications of Centre Manifold Theory*. Applied Mathematical Sciences **35**. Berlin: Springer-Verlag.
28. G. Iooss *Bifurcation of Maps and Applications*. Mathematics Studies **36**. Amsterdam: North-Holland. See pp. 201–222.

29. O. E. Landford 1973 *Bifurcation of Periodic Solution into Invariant Tori*: *the Work of Ruelle and Takrns*. Lecture Notes in Mathematics. Berlin: Springer-Verlag.
30. Y. H. Wan 1978 SIAM *Journal of Applied Mathematics* **1**, 34. Computation of the stability condition for the Hopf bifurcation of diffeomorphism on $R^2$.
31. K. Kaneko 1984 *Progress of Theoretical Physics* **72**, 202–215. Oscillation and doubling of torus.
32. A. Arneodo, P. H. Coullet and E. A. Spiegel 1983 *Physics Letters* **94**A, 1–6. Cascade of period doublings of tori.

## APPENDIX

Let us define the eigenvectors $\zeta_0$ and $\zeta_0^*$ such that

$$F_{01}\,\zeta_0 = \lambda_0\,\zeta_0, \qquad F_{01}^*\,\zeta_0^* = \overline{\lambda}_0\,\zeta_0^*, \qquad (\zeta_0, \zeta_0^*) = 1, \qquad (\overline{\zeta}_0, \zeta_0^*) = 0, \tag{A1}$$

where $F_{01} = Df(v_c, 0)$, $F_{01}^*$ is an adjoint of $F_{01}$ and (*, *) is the duality product between $E$ and its dual $E^*$. Then

$$\tilde{\lambda}_1 = (F_{11}(\zeta_0), \zeta_0^*), \qquad \left.\frac{\mathrm{d}|\lambda_1(v)|}{\mathrm{d}v}\right|_{v=v_c} = \mathrm{Re}(\tilde{\lambda}_1\,\mathrm{e}^{-\mathrm{i}\omega_0}), \tag{A2, A3}$$

$$g_{11} = \tfrac{1}{4}\left[\frac{\partial^2 F_1}{\partial y_1^2} + \frac{\partial^2 F_1}{\partial y_2^2} + \mathrm{i}\left(\frac{\partial^2 F_2}{\partial y_1^2} + \frac{\partial^2 F_2}{\partial y_2^2}\right)\right], \tag{A4}$$

$$g_{02} = \tfrac{1}{4}\left[\frac{\partial^2 F_1}{\partial y_1^2} - \frac{\partial^2 F_1}{\partial y_2^2} - 2\,\frac{\partial^2 F_2}{\partial y_1\,\partial y_2} + \mathrm{i}\left(\frac{\partial^2 F_2}{\partial y_1^2} - \frac{\partial^2 F_2}{\partial y_2^2} + 2\,\frac{\partial^2 F_1}{\partial y_1\,\partial y_2}\right)\right], \tag{A5}$$

$$g_{20} = \tfrac{1}{4}\left[\frac{\partial^2 F_1}{\partial y_1^2} - \frac{\partial^2 F_1}{\partial y_2^2} + 2\,\frac{\partial^2 F_2}{\partial y_1\,\partial y_2} + \mathrm{i}\left(\frac{\partial^2 F_2}{\partial y_1^2} - \frac{\partial^2 F_2}{\partial y_2^2} - 2\,\frac{\partial^2 F_1}{\partial y_1\,\partial y_2}\right)\right], \tag{A6}$$

$$G_{21} = \tfrac{1}{8}\left[\frac{d^3 F_1}{\partial y_1^3} + \frac{\partial^3 F_1}{\partial y_1\,\partial y_2^2} + \frac{\partial^3 F_2}{\partial y_1^2\,\partial y_2} + \frac{\partial^3 F_2}{\partial y_2^3} + \mathrm{i}\left(\frac{\partial^3 F_2}{\partial y_1^3} + \frac{\partial^3 F_2}{\partial y_1\,\partial y_2^2} - \frac{\partial^3 F_1}{\partial y_1^2\,\partial y_2} - \frac{\partial^3 F_1}{\partial y_2^3}\right)\right], \tag{A7}$$

$$H_{11}^{k-2} = \tfrac{1}{4}\left[\frac{\partial^2 F_k}{\partial y_1^2} + \frac{\partial^2 F_k}{\partial y_2^2}\right] \qquad (k = 3, 4), \tag{A8}$$

$$H_{20}^{k-2} = \tfrac{1}{4}\left[\frac{\partial^2 F_k}{\partial y_1^2} - \frac{\partial^2 F_k}{\partial y_2^2} - 2\mathrm{i}\,\frac{\partial^2 F_k}{\partial y_1\,\partial y_2}\right] \qquad (k = 3, 4), \tag{A9}$$

$$(I - D)W_{11} = H_{11}, \qquad (\overline{\lambda}^2 I - D)W_{02} = H_{02}, \tag{A10}$$

$$G_{10}^{k-2} = \tfrac{1}{2}\left[\frac{\partial^2 F_1}{\partial y_1\,\partial y_k} + \frac{\partial^2 F_2}{\partial y_2\,\partial y_k} + i\left(\frac{\partial^2 F_2}{\partial y_1\,\partial y_k} - \frac{\partial^2 F_1}{\partial y_2\,\partial y_k}\right)\right], \tag{A11}$$

$$G_{01}^{k-2} = \tfrac{1}{2}\left[\frac{\partial^2 F_1}{\partial y_1\,\partial y_k} - \frac{\partial^2 F_2}{\partial y_2\,\partial y_k} + i\left(\frac{\partial^2 F_2}{\partial y_1\,\partial y_k} + \frac{\partial^2 F_1}{\partial y_2\,\partial y_k}\right)\right] \qquad (k = 3, 4), \tag{A12}$$

$$g_{21} = G_{21} + \sum_{i=1}^{k-2} (2G_{10}^l\,W_{11}^l + G_{01}^l\,W_{20}^l), \tag{A13}$$

$$G_{30} = \tfrac{1}{8}\left[\frac{\partial^3 F_1}{\partial y_1^3} - 3\,\frac{\partial^3 F_1}{\partial y_1\,\partial y_2^2} + 3\,\frac{\partial^3 F_2}{\partial y_1^2\,\partial y_2} - \frac{\partial^3 F_2}{\partial y_2^3} + \mathrm{i}\left(\frac{\partial^3 F_2}{\partial y_1^3} - 3\,\frac{\partial^3 F_2}{\partial y_1\,\partial y_2^2} - 3\,\frac{\partial^3 F_1}{\partial y_1^2\,\partial y_2} + \frac{\partial^3 F_1}{\partial y_2^3}\right)\right], \tag{A14}$$

$$G_{03} = \tfrac{1}{8}\left[\frac{\partial^3 F_1}{\partial y_1^3} - 3\,\frac{\partial^3 F_1}{\partial y_1\,\partial y_2^2} - 3\,\frac{\partial^3 F_2}{\partial y_1^2\,\partial y_2} + \frac{\partial^3 F_2}{\partial y_2^3} + \mathrm{i}\left(\frac{\partial^3 F_2}{\partial y_1^3} - 3\,\frac{\partial^3 F_2}{\partial y_1\,\partial y_2^2} + 3\,\frac{\partial^3 F_1}{\partial y_1^2\,\partial y_2} - \frac{\partial^3 F_1}{\partial y_2^3}\right)\right], \tag{A15}$$

$$H_{30}^{k-2} = \tfrac{1}{8}\left[\frac{\partial^3 F_k}{\partial y_1^3} - 3\,\frac{\partial^3 F_k}{\partial y_1\,\partial y_2^2} + \mathrm{i}\left(\frac{\partial^3 F_k}{\partial y_2^3} - 3\,\frac{\partial^3 F_k}{\partial y_1^2\,\partial y_2}\right)\right], \tag{A16}$$

$$g_{30} = G_{30} + 3\sum_{l=1}^{k-2} G_{10}^{l}\, W_{20}^{l}, \qquad g_{03} = G_{03} + 3\sum_{l=1}^{k-2} G_{01}^{l}\, W_{02}^{l}. \tag{A17}$$